# Superconducting Properties of the Non-Fermi-Liquid System $\beta$-$YbAlB_4$

K. Kuga, Y. Karaki, Y. Matsumoto, Y. Machida, and S. Nakatsuji
*Institute for Solid State Physics (ISSP), University of Tokyo, Kashiwa 277-8581, Japan*
(Received 16 June 2008; published 26 September 2008)

$\beta$-$YbAlB_4$ is the first Yb-based heavy fermion superconductor with $T_c = 80$ mK. Our study using high-purity single crystals reveals that strongly type-II heavy fermion superconductivity emerges from the non-Fermi-liquid state with enhanced ferromagnetic fluctuations. High sensitivity of $T_c$ to sample purity indicates strong pair-breaking effects due to impurities, probably of nonmagnetic type, suggesting an unconventional character of the superconductivity.

DOI: 10.1103/PhysRevLett.101.137004 PACS numbers: 74.70.Tx, 74.25.Dw

Quantum criticality in correlated electron systems has attracted great interest because of the emergence of anomalous metallic, non-Fermi-liquid (NFL) properties that are quite different from those of ordinary metals [1–3]. It also promotes the emergence of superconductivity in the neighborhood of a quantum critical point (QCP), i.e., where a magnetic ordering temperature is driven to $T = 0$ K by tuning a physical parameter [4–6]. $4f$ intermetallic heavy fermion systems have provided a number of prototype materials for the study of such phenomena.

An important issue concerning $4f$ intermetallics is the possibility of the parallelism between the physical properties of electronlike ($4f^1$ Ce) and holelike ($4f^{13}$ Yb) compounds. The study of Ce and Yb materials indeed finds many similarities deriving from the antiferromagnetic coupling between the $4f$ magnetic moments and the conduction electrons (the Kondo screening) which leads to highly enhanced electronic effective masses at low temperatures [7]. There has been, however, a remarkable difference among their superconducting properties. While a number of Ce-based superconductors are found in the vicinity of an antiferromagnetic (AF) QCP [1–6], superconductivity in Yb-based heavy fermion compounds has never been reported until the recent discovery in the new compound $\beta$-$YbAlB_4$ [8].

$\beta$-$YbAlB_4$ is the first Yb-based heavy fermion superconductor with $T_c = 80$ mK [8]. Interestingly, the system exhibits pronounced NFL behavior in the normal state. The magnetic field dependence of the NFL behavior further indicates that $\beta$-$YbAlB_4$ is a rare example of a pure metal that is quantum critical without external tuning, i.e., without doping, applied pressure, and magnetic field [8]. Here, we report the superconducting properties of the NFL system $\beta$-$YbAlB_4$. Our study using high-purity single crystals indicates that the superconductivity in the clean limit emerges directly from the NFL state, most likely involving heavy quasiparticles. A divergent susceptibility indicates an existence of ferromagnetic fluctuations, in contrast with dominant AF fluctuations normally found in the Ce-based superconductors. Upper critical fields are anisotropic, and strongly suppressed for the field along the $c$ axis, possibly because of the paramagnetic effect due to the divergent $c$-axis susceptibility. Strong sensitivity of $T_c$ to sample purity suggests that the superconductivity is of an unconventional, non-$s$-wave type.

Single crystals of $\beta$-$YbAlB_4$ were prepared using the aluminum self-flux method [9]. Most single crystals form in a thin plate shape whose typical size is $\sim 1$ mm$^2$ $\parallel$ $ab$ plane $\times$ 0.01 mm $\parallel$ $c$ axis. An ac four-prove method has been employed for the transport measurements. Magnetization $M$ above 1.8 K was measured with a commercial SQUID magnetometer. For measurements down to 0.025 K, we employed a magnetometer made using dc-SQUID probes in conjunction with a dilution refrigerator. Earth's magnetic field was eliminated by using a Nb superconducting shield covered with a $\mu$-metal tube.

First, we present the superconductivity and NFL behavior found in the resistivity measurement. Figure 1(a) shows the resistivity plotted vs $T^{1.5}$ for single crystals with various quality. The sample A of the highest quality with a residual resistivity ratio, RRR $\sim 300$ and the residual resistivity $\rho(0) \sim 0.4$ $\mu\Omega$ cm has the highest $T_c$ of 80 mK. The resistance shows a sharp drop at $T_c$, and goes down to zero at 75 mK. Furthermore, the lower quality sample has the lower $T_c$ [inset of Fig. 1(a)]. Particularly, the sample C with the lowest RRR $\sim 70$ does not exhibit the superconductivity at least down to 30 mK, the lowest temperature of the measurement. On the other hand, the resistivity of all the samples shows $T^{1.5}$ dependence in the normal state below $\sim 1$ K. This suggests that the NFL behavior is fairly robust, and not so much dependent on the sample purity as the superconductivity.

To confirm the bulk nature of the superconductivity, we have performed the dc-SQUID magnetization measurements using a dozen of single crystals with RRR $> 200$ and an average RRR $\sim 240$. Figures 2(a) and 2(b) give the temperature dependence of the dc-susceptibility $M/H$ measured under a field $H$ along the $ab$ plane and the $c$ axis, respectively. A clear diamagnetic signal is observed in the susceptibility obtained through the zero-field-cooled (ZFC) sequence for both directions. Although the susceptibility for the field along the $ab$ plane does not reach the

 

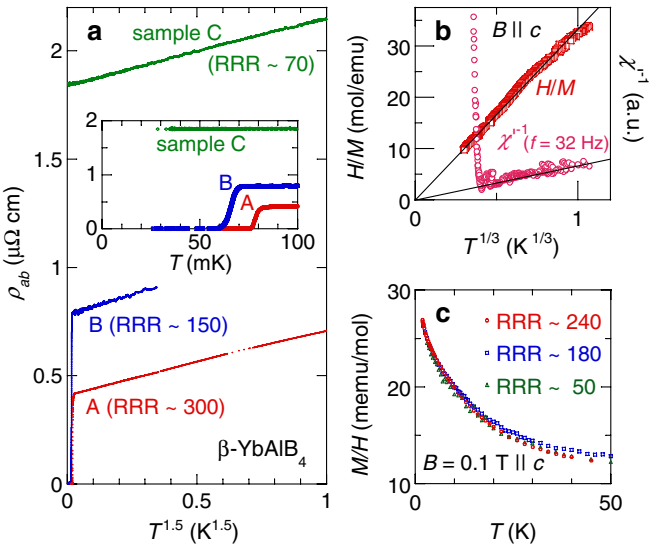


FIG. 1 (color online). (a) Zero-field in-plane resistivity $\rho_{ab}$ vs $T^{1.5}$ for various single crystals with different qualities. Inset: Temperature dependence of $\rho_{ab}$ for $T \leq 100$ mK. (b) Inverse dc susceptibility $H/M$ (left axis) and the inverse of the real part of the ac susceptibility $\chi'^{-1}$ (right axis) measured under a dc field of 12 mT along the $c$ axis are plotted vs $T^{-1/3}$. For the ac-susceptibility measurement, an ac field of 0.1 $\mu$T and the frequency $f = 32$ Hz is applied along the $c$ axis. The linear fits indicate a $T^{-1/3}$ dependence for the susceptibility. (c) Low temperature magnetic susceptibility measured under a field of 0.1 T along the $c$ axis for three sets of single crystals with different average RRR.

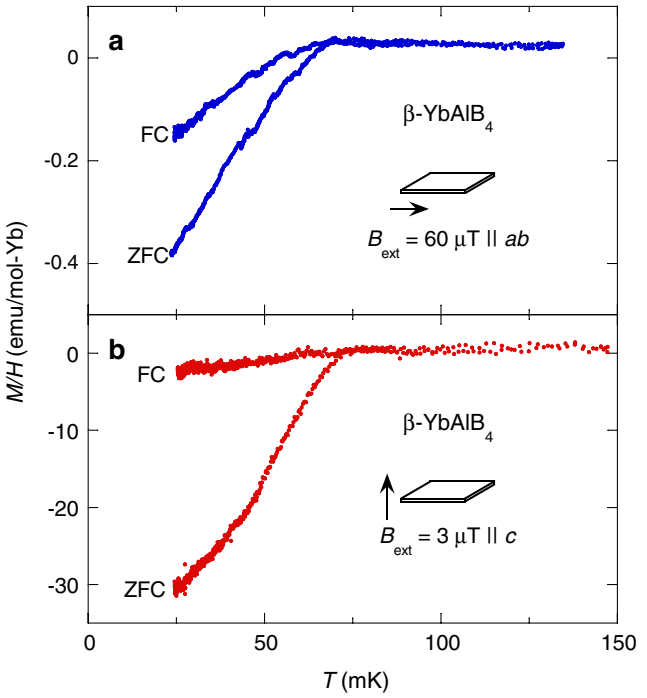


FIG. 2 (color online). Temperature dependence of the field-cooled (FC) and zero-field-cooled data (ZFC) of the dc susceptibility $M/H$, (a) under a field $H = 60$ $\mu$T along the $ab$ plane, and (b) under $H = 3$ $\mu$T along the $c$ axis.

full diamagnetic signal $-2.85$ emu/mol-Yb, the $c$-axis component well exceeds the full signal because of a large demagnetization effect. To estimate the demagnetization effect, we have also measured the superconducting diamagnetic signal of Al plates of similar size and geometry, and determined the average demagnetization factor $N$ to be $\sim 0$ for $B \parallel ab$ and $\sim 0.96$ for $B \parallel c$ axis. By making a comparison between voltage signals for Al plates and $\beta$-$YbAlB_4$ single crystals, we have estimated the volume fraction for the ZFC data at 25 mK, which reaches 15% for the field along the $ab$ plane and 40% for the field along the $c$ axis. The field-cooled (FC) data show a Meissner effect of 7% for the $ab$ plane and 6% for the $c$ axis, indicating a bulk superconductivity. For the $ab$-plane components, we have also confirmed almost the same volume fractions for both FC and ZFC sequences by normalizing the low $T$ voltage signal using the high $T$ magnetization data obtained using the commercial SQUID magnetometer. The relatively small Meissner effect for the field along the $c$ axis in comparison with the shielding effect should be due to the trapping of magnetic field flux perpendicular to the sample plate. On the other hand, for the field along the $ab$ plane, the observed value is actually as large as the full volume fraction estimated considering the field penetration depth. The penetration depth $\lambda_c$ along the $c$ axis is long $\sim 7.5$ $\mu$m, as we will discuss later, and comparable with the sample thickness along the $c$ axis ($\sim 10$ $\mu$m). Thus, the field penetration should diminish the apparent volume fraction down to $\sim 15\%$ for the field along the $ab$ plane, which is consistent with our observation. The $T$ dependence of the diamagnetism is rather broad because of (1) the distribution of $T_c$ among the samples, (2) the long penetration depth, and (3) the temperature dependence of the demagnetization effect for the $c$-axis component.

As in the cases of the resistivity, the temperature dependence of the magnetic susceptibility in the normal state shows a clear NFL behavior. In Fig. 1(b), we show the temperature dependence of the inverse dc-susceptibility $H/M$ and the inverse of the real part of the ac-susceptibility $\chi'^{-1}$ measured in the FC sequence under a field along the $c$ axis. Here, the field $\mu_0 H$ of 12 mT is applied to obtain a sizable dc voltage output. Although the Meissner effect in the dc magnetization is not clearly observed because of pinning effect, the superconducting transition can be seen as the onset of the sharp drop of the ac susceptibility. The normal state susceptibility is found to systematically increase on cooling as a linear function of $T^{-1/3}$ below $\sim 1$ K and down to $T_c \sim 60$ mK. This diverging behavior, consistent with the results obtained by the Faraday method [8], indicates a significant role of ferromagnetic fluctuations in the NFL behavior.

The field dependence of the magnetization in the superconducting state is also obtained using the dc-SQUID

probe. For each measurement, the samples were first cooled down to 25 or 30 mK from the normal state in zero field (the residual magnetic field below ~0.6 $\mu$T). Then, the field was increased up to a certain field and decreased back to zero to obtain a magnetization curve. Figure 3(a) presents the magnetization curve measured under field up to ~1.2 mT along the $ab$ plane. The lower critical field $B_{c1\|ab}$ is estimated to be ~28 $\mu$T at which the low field $M$ starts to deviate from the initial linear response [inset of Fig. 3(a)]. For $B \parallel c$, the field was increased up to ~60 $\mu$T, as shown in Fig. 3(b). $M$ shows a deviation from a linear decrease at ~4 $\mu$T, and thus, $B_{c1}$ for $B \parallel c$ should be roughly ~0.1 mT, given that the demagnetization factor $N \sim 0.96$.

The $M$ vs $B$ curves for both field directions show clear hystereses as flux pinning effects. Generally, by analyzing a hysteresis curve, an order of magnitude of the critical current density $J_c$ may be estimated. Using the Bean model [10,11], $J_c$ under the field along the $ab$ plane is given by the formula $J_c = 4(M_\uparrow - M_\downarrow)/d$. Here, we assume a slab shape sample with a thickness $d$. $M_\uparrow$ and $M_\downarrow$ are the magnetizations in the sequences of increasing and decreasing field, respectively. Using the results in the main panel of Fig. 3(a) as well as a typical thickness of the sample, $d = 0.01$ mm, $J_c$ is evaluated to be ~300 A/cm$^2$. For the field along the $c$ axis, the critical current along the $ab$ plane can be estimated using the formula $J_c^{ab} = 30(M_\uparrow - M_\downarrow)/t$ [12]. Here, we assume that the field is applied perpendicular to a thin square sample with a side length of $t$. Using the results in Fig. 3(b) as well as a typical size of the sample, $t = 1$ mm, $J_c^{ab}$ is evaluated to be >500 A/cm$^2$.

The suppression of the superconductivity under field is investigated by measurements of the in-plane resistivity at fixed temperatures or fields. Figure 4 presents the temperature dependence of the upper critical field $B_{c2}$. Different crystals with similar $T_c$ (81 and 77 mK) were employed for the measurements under field along the $ab$ plane and the $c$ axis. The critical field is defined as the onset of the transition as shown in the inset of Fig. 4. The ac-susceptibility measurements at constant temperatures yield the results consistent with the resistivity measurements (not shown). $B_{c2}$ is anisotropic and by extrapolating its temperature dependence we can roughly estimate the zero temperature values, $B_{c2}(0) \sim 150$ mT for $B \parallel ab$ plane, and 25 mT for $B \parallel c$ axis. Furthermore, the $B_{c2}$ curves have a rather large gradient at $T_c$, $B'_{c2} \equiv dB_{c2}/dT \approx -2.6$ T/K for $B \parallel ab$ plane, and $-1.4$ T/K for $B \parallel c$ axis.

Orbital critical fields can be evaluated based on the Werthamer-Helfand-Hohenberg (WHH) model as broken curves shown in Fig. 4 [13]. The model estimates the orbital critical field at absolute zero to be $B_{c2}^{\mathrm{orb}}(0) = 0.727 B'_{c2} T_c \sim 150$ mT for $B \parallel ab$ plane and 76 mT for

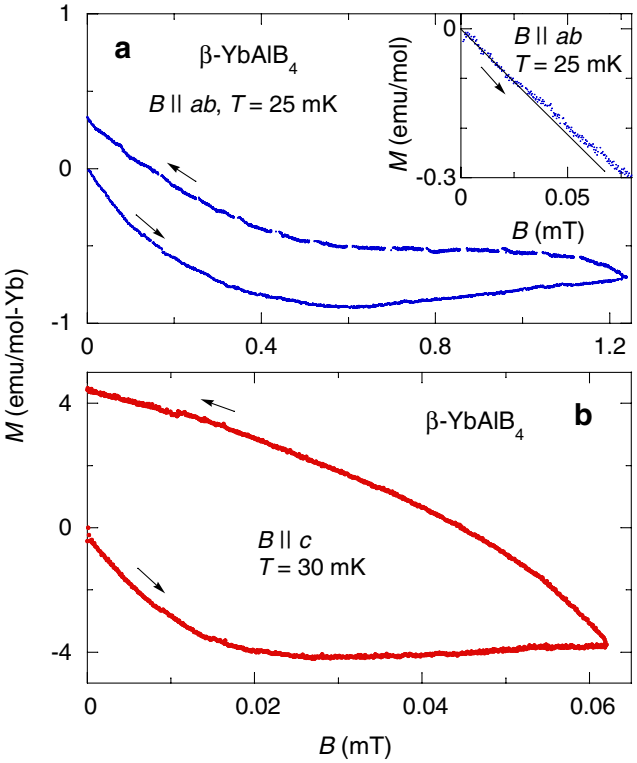


FIG. 3 (color online). $M$ vs $B$ in the superconducting state of $\beta$-YbAlB$_4$ under the field (a) along the $ab$ plane at 25 mK, and (b) along the $c$ axis at 30 mK. Inset: (a) Low field part of the magnetization curve in the main panel.

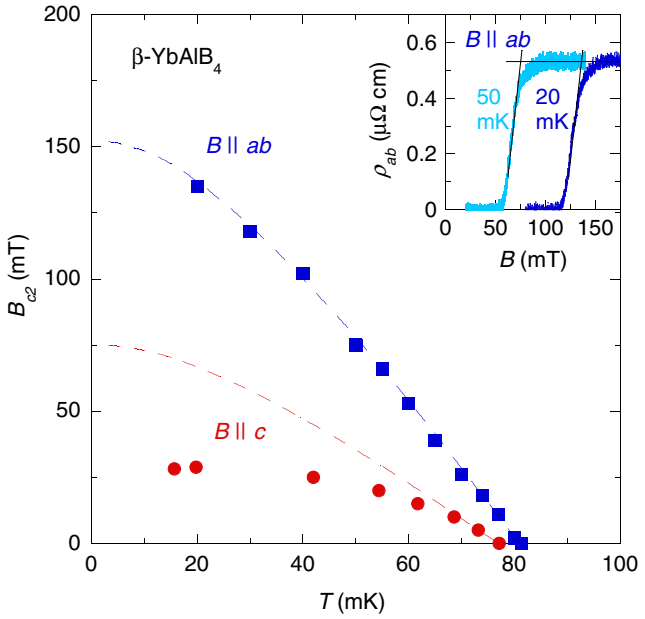


FIG. 4 (color online). Temperature dependence of the upper critical field $B_{c2}$ along the $ab$ plane (square, blue) and the $c$ axis (circle, red). Different single crystals with similar $T_c$ were used for each field direction measurement. Broken lines represent the curves obtained by fitting to the experimental results near $T_c$ using the WHH model. Inset: In-plane resistivity $\rho_{ab}$ vs $B$. $B_{c2}$ is defined as the crossing point of the linear extrapolation lines of the resistivity in the normal state and the resistivity change in the transition.

$B \parallel c$ axis. For the field along the $ab$ plane, the overall feature of the curve is consistent with experiment. For the field along the $c$ axis, however, the curve obtained from the WHH model shows a clear deviation from experiment, giving about 3 times higher values at $T \to 0$.

The Pauli limit due to the paramagnetic effect, on the other hand, is generally given by $B_{c2}^{\mathrm{Pauli}}(0) = 1.83T_c$ for a weak coupling spin-singlet superconductor [14]. This yields $B_{c2}^{\mathrm{Pauli}}(0) \sim 0.15$ T for $T_c = 80$ mK of $\beta$-$YbAlB_4$, which is still 6 times larger than $B_{c2}(0)$ for $B \parallel c$. Taking account of the divergent Ising magnetization, this simple estimate of $B_{c2}^{\mathrm{Pauli}}(0)$ should not work for this system. The strong suppression of $B_{c2\|c}$ in comparison with $B_{c2}^{\mathrm{orb}}(0)$ might be due to the paramagnetic effect enhanced by the large Ising magnetization along the $c$ axis.

The knowledge of the critical fields allows us to estimate superconducting parameters using the Ginzburg-Landau (GL) formula for an anisotropic three-dimensional superconductor. The equations, $B_{c2\|c} = \Phi_0/(2\pi\xi_{ab}^2)$ and $B_{c2\|ab} = \Phi_0/(2\pi\xi_{ab}\xi_c)$ yield the coherence lengths $\xi_{ab}(0) = 66$ nm and $\xi_c(0) = 33$ nm. Here, we take the orbital critical fields $B_{c2}^{\mathrm{orb}}(0)$ as the estimates for $B_{c2}$. Given $B_{c1\|ab} = 28$ $\mu$T, and using the formula $B_{c2} = \sqrt{2}\kappa B_c$ and $B_{c1}B_{c2} = B_c^2(\ln\kappa + 0.08)$, the thermodynamic critical field $B_c$ and the GL parameter $\kappa$ can be estimated as $B_c = 0.93$ mT, $\kappa_{ab} = 110$ and $\kappa_c = 58$. Finally, the relations, $\kappa_c = \lambda_{ab}/\xi_{ab}$ and $\kappa_{ab} = (\lambda_{ab}\lambda_c/(\xi_{ab}\xi_c))^{1/2}$ yield the penetration lengths of $\lambda_{ab} = 3.8$ $\mu$m and $\lambda_c = 7.5$ $\mu$m.

The physical parameters can be also estimated, following the BCS theory [15,16]. To simplify the calculation, we assume a spherical Fermi surface with a Fermi wave number $k_{\mathrm{F}}$. By using the knowledge that $B'_{c2} = -2.6$ T/K, the residual resistivity $\rho(0) = 0.4$ $\mu\Omega$ cm, and the electronic specific heat coefficient $\gamma = 150$ mJ/mol K$^2$, we estimate $k_{\mathrm{F}} = 4.6 \times 10^9$ 1/m, the mean free path $l = 1.5$ $\mu$m, the coherence length $\xi_0 = 52$ nm, and the penetration depth $\lambda = 1.2$ $\mu$m. Notably, both $\xi_0$ and $\lambda$ are roughly consistent with the values obtained by the GL equations above. Furthermore, our results indicate that $l$ is 2 orders of magnitude longer than $\xi_0$ and thus the superconductivity is within the clean limit. One can also calculate the effective mass $m^*/m_0$ to be $\sim$180. This large $m^*/m_0$ as well as $\gamma$ indicates the heavy fermion nature of the superconductivity.

Finally, we discuss the strong sensitivity of the superconductivity to sample purity. As shown in the inset of Fig. 1(a), a sample with the higher $\rho(0)$ has the lower $T_c$. Particularly, the sample C with $\rho(0) \sim 2$ $\mu\Omega$ cm has $T_c < 30$ mK. Given $k_{\mathrm{F}} = 4.6 \times 10^9$ 1/m, the sample C has $l \sim 0.27$ $\mu$m, which is only 4 times longer than $\xi_{ab}(0)$. This indicates that the superconductivity appears only in the clean limit. We have also performed the low temperature magnetic susceptibility measurements down to 2 K for three sets of single crystals with different average RRR between 50 and 240 [Fig. 1(c)]. The data for all the samples collapse on top of each other and follow almost the same curve down to 2 K, indicating that the impurity is most likely nonmagnetic. The strong pair-breaking nature against nonmagnetic impurities suggests an unconventional superconductivity of $\beta$-$YbAlB_4$.

To conclude, our study on the superconducting properties of the first Yb-based heavy fermion superconductor $\beta$-$YbAlB_4$ with $T_c = 80$ mK reveals strongly type-II heavy fermion superconductivity in the clean limit. The upper critical fields are anisotropic and likely have a paramagnetic effect for the field along the $c$ axis. Strong pair-breaking nature most likely due to the nonmagnetic impurities suggests that $\beta$-$YbAlB_4$ is an unconventional, non-$s$-wave superconductor. Interestingly, the superconductivity directly emerges from the NFL state with enhanced ferromagnetic fluctuations. This is in contrast with the superconductivity in the Ce-based compounds that are normally found close to AF QCPs. The effect of the ferromagnetic fluctuations on the superconductivity and its pairing symmetry is an interesting issue for future investigation.

We thank S. Yonezawa, H. Takatsu, Y. Maeno, and H. Ishimoto for their support in many aspects and Y. Yanase, K. Miyake, T. Tomita, T. Sakakibara, K. Ueda, D. F. Agterberg, and T. Dahm for useful discussions. This work has been supported in part by Grants-in-Aid for Scientific Research from JSPS, Grant-in-Aid for Scientific Research on Priority Areas from MEXT of Japan.

[1] G. R. Stewart, Rev. Mod. Phys. **73**, 797 (2001).
[2] H. v. Löhneysen, A. Rosch, M. Vojta, and P. Wölfle, Rev. Mod. Phys. **79**, 1015 (2007).
[3] P. Gegenwart, Q. Si, and F. Steglich, Nature Phys. **4**, 186 (2008).
[4] P. Monthoux, D. Pines, and G. G. Lonzarich, Nature (London) **450**, 1177 (2007).
[5] N. D. Mathur *et al.*, Nature (London) **394**, 39 (1998).
[6] H. Q. Yuan *et al.*, Science **302**, 2104 (2003).
[7] A. C. Hewson, *The Kondo Problem to Heavy Fermions* (Cambridge Univ. Press, Cambridge, 1993).
[8] S. Nakatsuji *et al.*, Nature Phys. **4**, 603 (2008).
[9] R. T. Macaluso *et al.*, Chem. Mater. **19**, 1918 (2007).
[10] C. P. Bean, Rev. Mod. Phys. **36**, 31 (1964).
[11] A. Pollini *et al.*, J. Low Temp. Phys. **90**, 15 (1993).
[12] E. M. Gyorgy *et al.*, Appl. Phys. Lett. **55**, 283 (1989).
[13] E. Helfand and N. R. Werthamer, Phys. Rev. **147**, 288 (1966).
[14] A. M. Clogston, Phys. Rev. Lett. **9**, 266 (1962).
[15] T. P. Orlando *et al.*, Phys. Rev. B **19**, 4545 (1979).
[16] U. Rauchschwalbe *et al.*, Phys. Rev. Lett. **49**, 1448 (1982).